

Received:
11 November 2019

Revised:
03 January 2020

Accepted:
17 February 2020

Cite this article as:

Sartoretti E, Sartoretti T, Gutzwiller A, Karrer U, Binkert C, Najafi A, et al. Advanced multimodality MR imaging of a cerebral nocardiosis abscess in an immunocompetent patient with a focus on Amide Proton Transfer weighted imaging. *BJR Case Rep* 2020; **6**: 20190122.

CASE REPORT

Advanced multimodality MR imaging of a cerebral nocardiosis abscess in an immunocompetent patient with a focus on Amide Proton Transfer weighted imaging

¹ELISABETH SARTORETTI, ¹THOMAS SARTORETTI, ²ANNINA GUTZWILLER, MD, ²URS KARRER, MD, PhD, ¹CHRISTOPH BINKERT, MD, ¹ARASH NAJAFI, MD, ³DAVID CZELL, MD, ¹SIMON BEYELER and ¹SABINE SARTORETTI-SCHEFER, MD

¹Institut für Radiologie, Kantonsspital Winterthur, Brauerstrasse 15, 8401 Winterthur, Switzerland

²Klinik für Innere Medizin, Kantonsspital Winterthur, Brauerstrasse 15, 8401 Winterthur, Switzerland

³Klinik für Innere Medizin, Zuger Kantonsspital, Landhausstrasse 11, 6340 Baar, Switzerland

Address correspondence to: Dr Sabine Sartoretti-Schefer
E-mail: sabine.sartoretti@ksw.ch

ABSTRACT

Cerebral nocardiosis abscess is a very rare entity in an immunocompetent patient. In this case report multiparametric and multimodality MR imaging characteristics of a pyogenic brain abscess caused by *Nocardia Farcinica* are discussed with a specific focus on amide proton transfer weighted imaging as a modern non-invasive, molecular MR imaging method which detects endogenous mobile protein and peptide concentration and tissue pH changes in pathologic brain lesions. The imaging characteristics are reviewed and discussed in respect to possible differential diagnoses, especially malignant tumorous lesions.

INTRODUCTION

Nocardia is a Gram-positive bacillus, that causes cutaneous, ocular and central nervous system (CNS) infections especially in immunocompromised patients with deficiencies in the cell-mediated immunity.¹ CNS infections (meningitis and rarely brain abscess) occur in 9–44% of these patients.^{1,2} However, in general, nocardial brain abscesses appear very rarely and only represent^{1,2} 1–2% of all brain abscesses.³

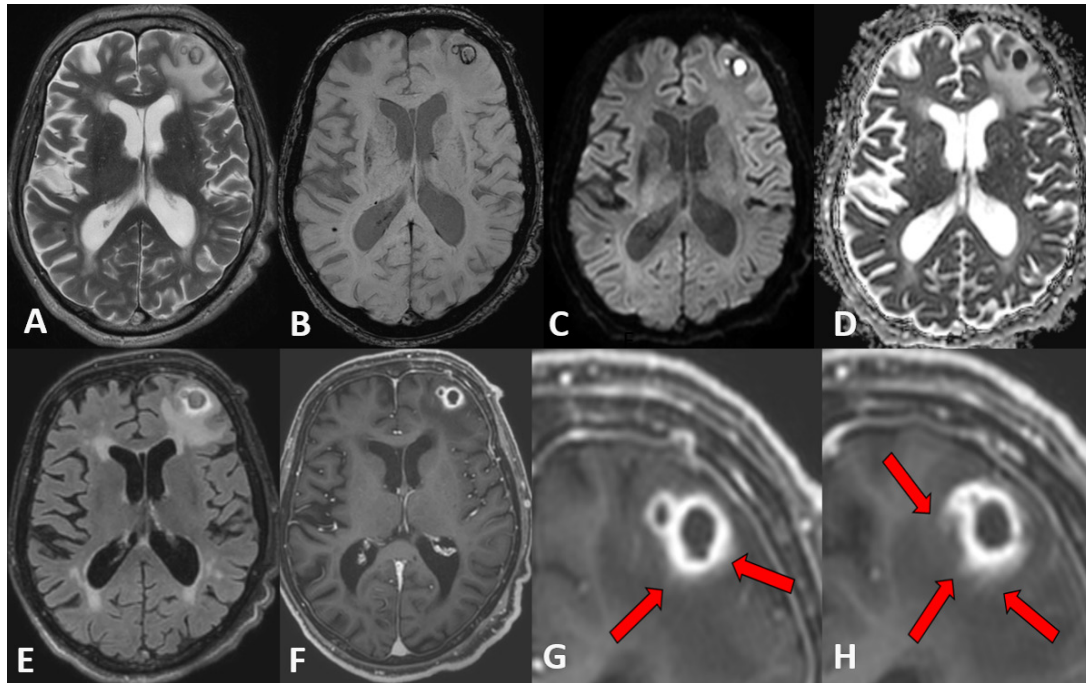
In our report, we describe a rare case of a brain abscess due to *Nocardia Farcinica* in an immunocompetent patient. The patient was referred to the emergency unit after an epileptic seizure. CT imaging showed a tumorous frontal mass lesion. In our department, all patients with brain tumors are examined with an advanced comprehensive multimodal brain MRI imaging protocol^{4–6} for further characterization of the tumorous lesion. This protocol consists of morphological MR sequences (T_2 weighted (T_2W) turbo spin echo (TSE), T_1W pre-contrast turbo field echo (TFE), post-contrast T_1W m-Dixon TFE, three-dimensional fluid attenuated inversion recovery (FLAIR), diffusion weighted imaging (DWI), susceptibility weighted imaging (SWI)) and of

advanced imaging modalities (Diffusion tensor imaging (DTI), dynamic susceptibility contrast (DSC) perfusion-weighted imaging (PWI), dynamic contrast enhanced (DCE) PWI, single voxel spectroscopy and amide proton transfer weighted (APT_w) imaging).

On morphological MRI (DWI, SWI, T_2W and post-contrast T_1W imaging) as well as on advanced MR imaging based on DSC PWI and DTI the frontal mass lesion could be diagnosed as a brain abscess although spectroscopy data and k-trans values resulting from DCE PWI were inconclusive. The diagnosis of brain abscess caused by *Nocardia farcinica* was finally confirmed following neurosurgical intervention.

While the imaging characteristics of *Nocardia* brain abscesses are well known for certain standard imaging modalities such as DWI or DSC, the imaging characteristics on APT_w images have not been described to this date. With APT_w imaging being a modern non-invasive, molecular MRI method that has shown promise in imaging tumors and infective mass lesions,⁷ a detailed description of these imaging characteristics may be of interest as APT_w imaging may become a valuable future asset in imaging infective

Figure 1. Transverse T_2W TSE (A), SWI (Figure 1B), DWI (Figure 1C), ADC map (Figure 1D) and FLAIR (Figure 1E) images and post-contrast T_1W TFE (Figure 1F–1H) presenting the two peripherally contrast enhancing confluent lesions in the left frontal white matter. Red arrows show indistinct contrast enhancement in the surrounding tissue. ADC, apparent diffusion coefficient; DWI, diffusion-weighted imaging; FLAIR, fluid attenuated inversion recovery; SWI, susceptibility-weighted imaging; T_2W , T_2 weighted; TFE, turbo field echo.



mass lesions especially in complex cases where the diagnosis can not be ascertained with currently available imaging modalities.

CASE REPORT

A 76-year-old patient with chronic obstructive pulmonary disease, chronic atrial fibrillation and alcohol overconsumption was admitted to the hospital in a soporous to comatose state (Glasgow coma scale GCS 5) after persistent focal-complex epileptic seizures. On emergency CT imaging, a focal peripherally contrast enhancing mass lesion in the frontal lobe on the left side was detected. Advanced multimodal brain tumor imaging was performed for further characterization of the tumorous lesion.

On morphological brain MRI (Figure 1), two confluent and centrally necrotic lesions (of 7 and 14mm diameter) with peripheral irregular contrast enhancing rims (Figure 1F–H), hypointense on T_2W TSE (Figure 1A) and with double rim sign on SWI (Figure 1B), and with substantial perifocal edema on FLAIR (Figure 1E) and T_2W images (Figure 1A) were visible in the left middle frontal gyrus. On SWI (Figure 1B), the outer hypointense rims were irregular with central hypointense protrusions. The contrast enhancing rims (Figure 1F–H) were thick and irregular, hyperintense on FLAIR (Figure 1E), without well-delineated borders and with slight DCE in the surrounding tissue (red arrows in Figure 1G–H).

On DSC perfusion, the relative cerebral blood volume of the contrast enhancing rim compared to normal white matter in

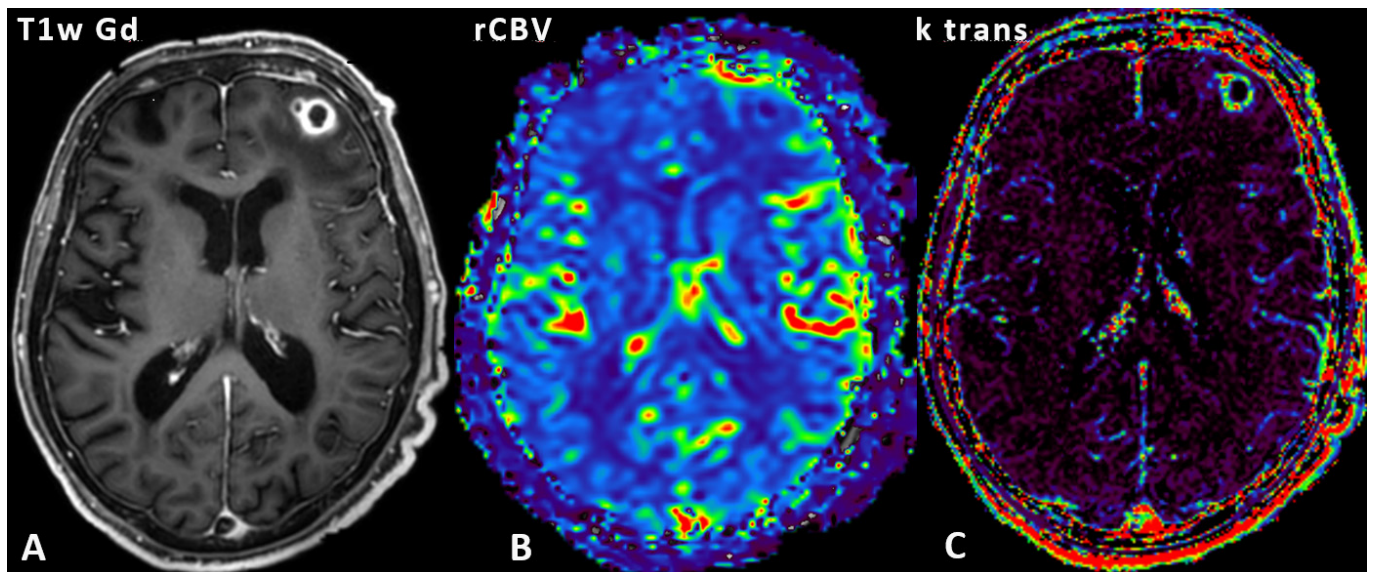
the centrum semiovale (rCBV) was not pathologically increased (Figure 2A and B) with a rCBV of 0.86. On DCE perfusion, the k-trans values of the contrast enhancing rim were evaluated (Figure 2C) and varied between 22 and $41 \times 10^{-3}/\text{min}$ compared to a value of $2.3 \times 10^{-3}/\text{min}$ of normal contralateral white matter. A high signal intensity increase on DCE perfusion lead to a maximum relative enhancement of 81% compared to 4.6% of normal white matter resulting in an ascending curve without wash-out.

The necrotic center presented with homogeneous hyperintensity on DWI (Figure 1C) and with severely reduced apparent diffusion coefficient (ADC) (Figure 1D) corresponding to diffusion restriction with a mean ADC value of $0.4 \times 10^{-3} \text{ mm}^2/\text{s}$ and with a central fractional anisotropy (FA) value of 0.28 on DTI.

Single voxel spectroscopy with a voxel size of 16 mm^2 and an echo time (TE) of 30 ms centered on the two lesions presented with a very high lipid peak (Lip/Cr ratio of 11.8), with a small lactate peak (Lac/Cr 0.316) with a decreased NAA (NAA/Cr ratio 1.51) and with slightly increased Cholin (Cho/Cr ratio 1.12 and Cho/NAA ratio 0.741) (Figure 3). Myoinositol and acetate were not elevated.

Morphological characteristics on DWI, SWI, T_2W and post-contrast T_1W images together with decreased rCBV in the contrast enhancing rim on DSC PWI and high FA value within the central necrosis on DTI ascertained the diagnosis of pyogenic brain abscess.

Figure 2. DSC perfusion with rCBV map: A T_1W TFE m-Dixon transverse image (Figure 2A) is overlaid on the rCBV map (Figure 2B). The k-trans map is visible in Figure 2C. The contrast enhancing rim does not show any hyperperfusion. DSC, dynamic susceptibility contrast; T_1W , T_1 weighted; TFE, turbo field echo.



APT_w images were overlaid, fused and coregistered with a T_1W TFE post-contrast image on a separate workstation (Intellispace Portal[®] Philips version 8) (Figure 4). This procedure allowed to switch from the T_1W post-contrast TFE image (Figure 4A) to the mixed T_1W / APT_w image (each 50%, on Figure 4B) to the pure APT_w image (Figure 4C). Free hand regions of interest (ROIs) were drawn on the T_1W post-contrast TFE sequence and APT_w values were obtained on the fused APT_w image. The ROIs were drawn within the necrotic center, in the contrast enhancing rim, in the surrounding edema directly adjacent to the contrast enhancing rim, in the surrounding edema at approximately 1 cm distance to the contrast enhancing rim and in the normal frontal white matter (Figure 5). To assess the APT_w values of the whole contrast enhancing rim, a voxelwise segmentation was performed on APT_w images fused with postcontrast TFE images on a separate workstation (Intellispace Discovery[®] Philips Healthcare,

Best, the Netherlands). Based on the segmentation data, a histogram was then computed with the statistical programming language “R v3.6.1” in the “R Studio” environment in combination with the packages “ggplot2” and “cowplot” (Figure 6).

The necrotic center had APT_w values of 2.6%/2.3%/2.1% (maximum/mean/minimum), the directly surrounding edema had values of 3.3%/2.9%/2.2% , the more distant edema had values of 2.4%/2.0%/1.6% and the normal white matter had values of 1.4%/1.2%/0.9% (Figure 5). From the histogram of APT_w values of the entire contrast enhancing rim (Figure 6), the following precise parameters were derived: minimum = 1.9%, 25th percentile = 2.4%, median = 2.6%, mean = 2.6%, 75th percentile = 2.9%, maximum = 3.1%, thus corresponding approximately to the APT_w values of the contrast enhancing rim, obtained by manual ROI measurements (Figure 5) (with APT_w

Figure 3. Single voxel spectroscopy with a voxel of 16 mm³ centered on the brain abscess.

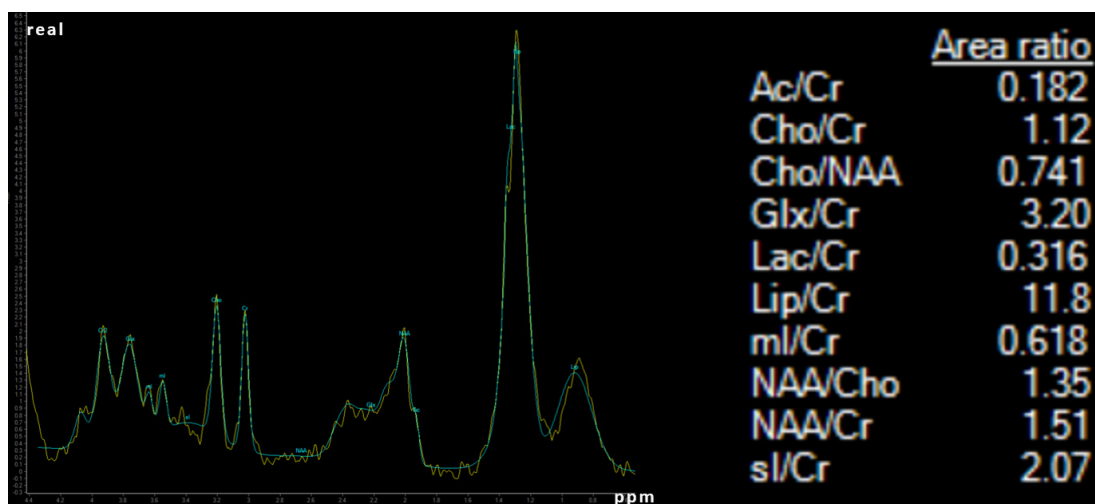
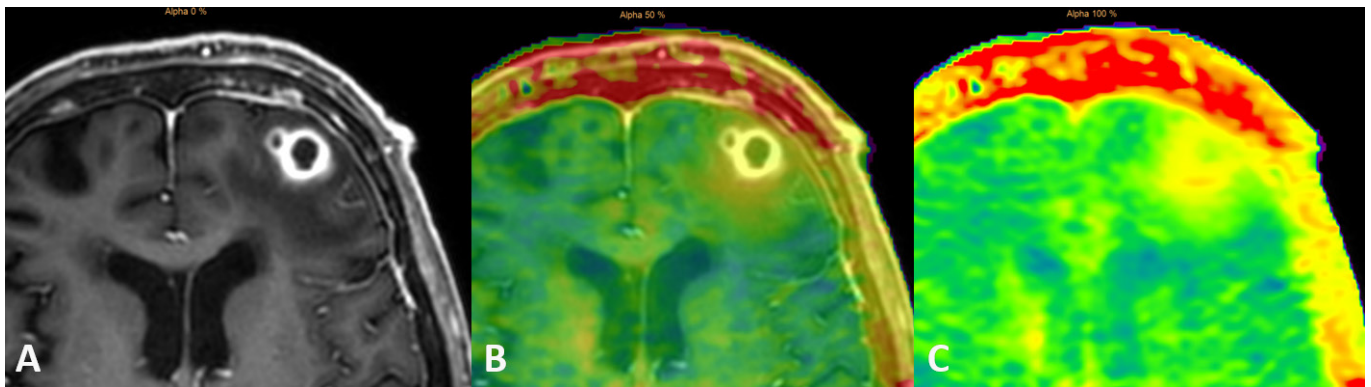


Figure 4. Postcontrast T_1W TFE image (Figure 4A) overlaid on the APTw image (Figure 4B) and pure APTw image (Figure 4C). APTw,amide proton transfer weighted; T_1W , T_1 weighted; TFE, turbo field echo.



3.1–3.3% / 2.5–2.8% / 2.2–2.5%). Additionally, two distinct peaks within the contrast enhancing rim were observed at 2.4 and 2.9% (Figure 6).

Following MR imaging, neurosurgical abscess aspiration of pus was performed and empirical treatment with Ceftriaxone, Metronidazole, Dexamethasone was started. Microscopy of the abscess

showed filamentous Gram-positive rods. *Nocardia Farcinica* was identified on cultures by 16S-rRNA sequencing. Treatment was adjusted to Imipenem and Trimethoprim- Sulfomethoxazol (TMP-SXT). Additional work-up excluded overt immunosuppression and additional infectious foci, especially in the lungs. Due to severe side-effects of antibiotic therapy with renal failure, nausea, weight loss, TMP- SXT had to be discontinued and

Figure 5. APTw values within the central necrosis, the contrast enhancing rim, the direct perifocal edema with inflammatory tissue (cerebritis) and the distant surrounding edema compared to APTw values of normal frontal white matter. APTw, amide proton transfer weighted.

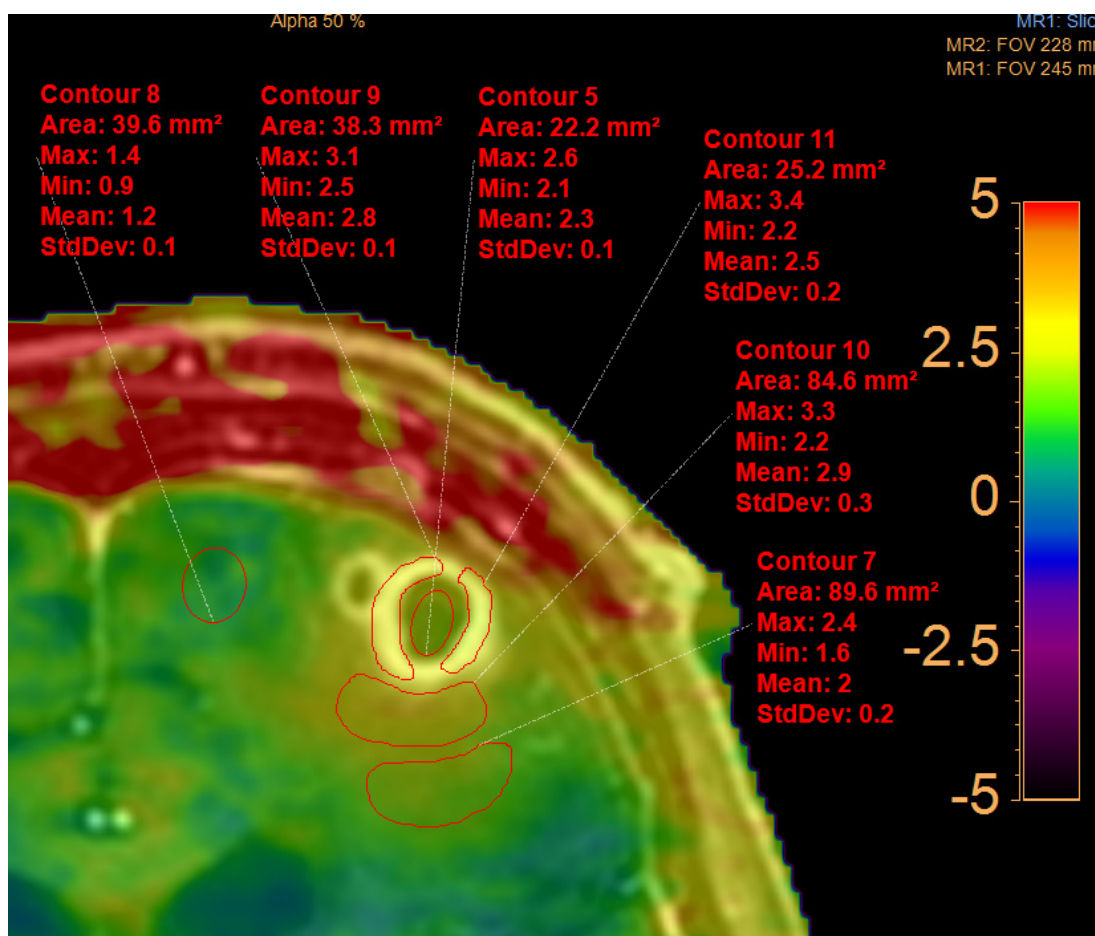
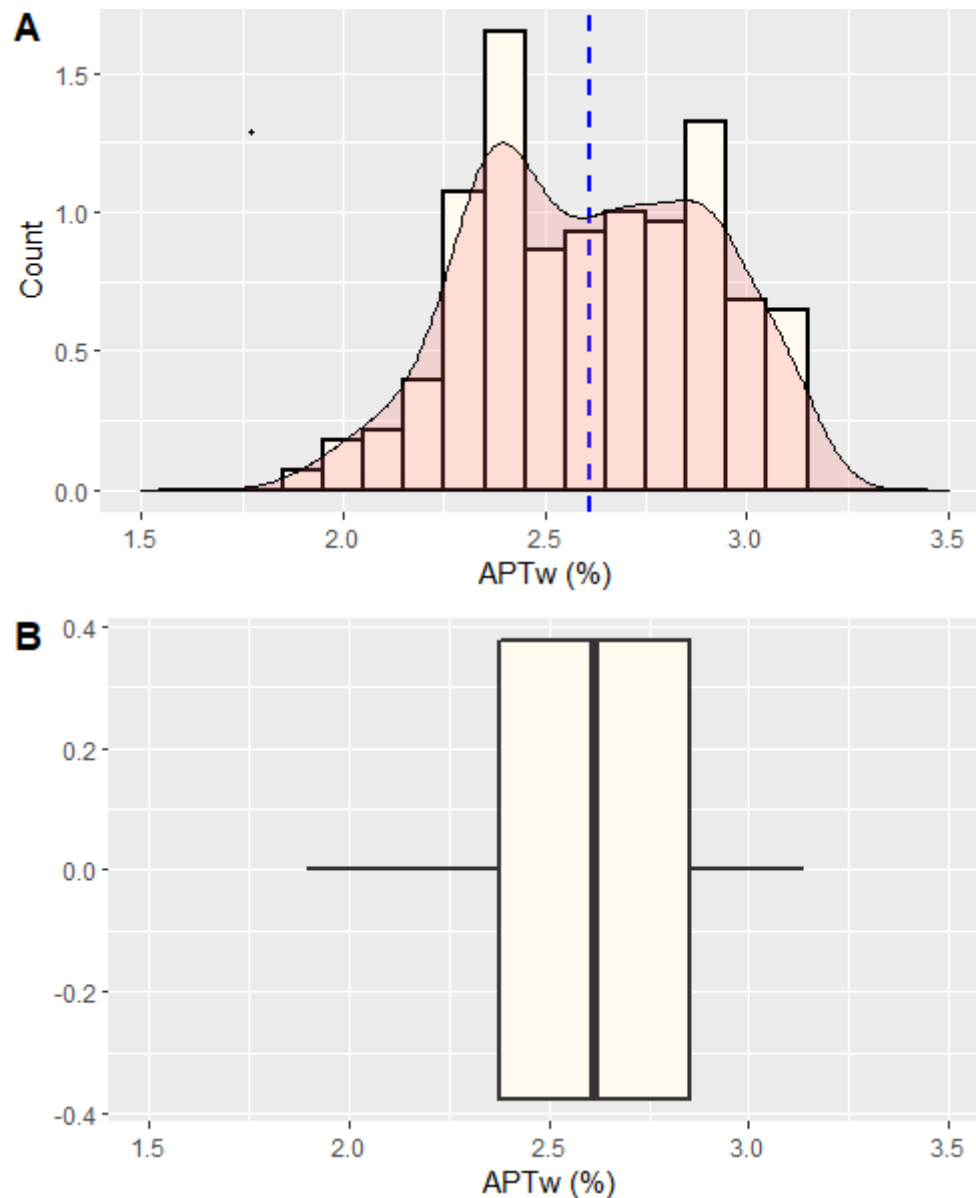


Figure 6. Histogram of the contrast enhancing rim. The histogram was computed with the statistical programming language “R v3.6.1” in the “R Studio” environment in combination with the packages “ggplot2” and “cowplot”. Figure 6A shows the histogram with an overlaid density plot in red. The mean is depicted as a dashed blue line. It presents a double peak with APTw values at 2.4% and 2.9% Figure 6B shows a boxplot of the data with the median as a prominent black line in the middle and the 25th and 75th percentile as the outer borders of the box. APT, amide proton transfer.



Meropenem was started. The patient's condition deteriorated and he died of respiratory failure on the 11th day after hospital admission.

The patient gave general written informed consent after admission to the hospital.

DISCUSSION

In this report, we describe the MR imaging findings of a cerebral Nocardiosis abscess in an immunocompetent patient and specifically provide previously unpublished APTw imaging characteristics. Lastly, we discuss the imaging findings in respect to possible

differential diagnoses such as high grade tumorous brain lesions (*i.e.* high grade glioma and cerebral metastasis).

Nocardiosis is a localized or disseminated infection caused by *Nocardia*, an aerobic actinomycete with multiple species.^{8–10} The majority of *Nocardia* infections occur in patients with cell-mediated immunosuppressive conditions; however, up to 50% of patients with nocardial infections are immunocompetent.^{3,10} *Nocardia* brain infection can occur as an isolated¹⁰ or as a disseminated disease in two or more organs, especially with involvement of lungs, skin and brain.^{3,8} CNS infection occurs in up to 44% of patients with Nocardiosis,³ mostly presenting as meningitis and

very rarely as brain abscess.^{1,2} Our patient was diagnosed with brain abscess due to *Nocardia farcinica*. This species has a higher risk for dissemination to the brain than other *Nocardia* species,⁸ but brain abscesses are rare, often multifocal, poorly encapsulated, mostly located in frontal and parietal lobes^{2,3,8} and present with a very high mortality rate between 30 and 60%^{2,3,8} because the germ is often resistant to multiple antibacterial agents.¹⁰ A combined immediate approach of medical and surgical therapy is recommended.^{3,8,10}

On MRI, the diagnosis of a pyogenic brain abscess could be established based on morphological MR imaging with central diffusion restriction on DWI, T1 hypointense rim, double rim sign on SWI, peripheral rim enhancement on T₁W TFE images.¹¹

Multimodality DSC PWI and DTI imaging confirmed the diagnosis of brain abscess with hypoperfusion/low rCBV of the contrast enhancing rim compared to normal white matter^{12,13} and with high FA values within the central necrosis.¹⁴ Nonetheless, certain imaging findings pointed towards a malignant brain tumor. Specifically, spectroscopy presented with a very high lipid peak and elevated cholin peak corresponding to a spectrum of a malignant tumor^{13,15,16}; peaks specific for brain abscess as succinate at 2.4 ppm, acetate at 1.9 ppm, alanine at 1.5 ppm, aminoacids at 0.9 ppm and lactate at 1.3 ppm were absent.¹⁵⁻¹⁷ The perfusion parameters obtained by DCE perfusion (especially k-trans values and perfusion time curves) were also mimicking the appearance of tumorous lesions.¹⁸⁻²⁰

Thus, to summarize, the imaging results from routine multimodality and multiparametric imaging (DTI, DSC, DCE perfusion and spectroscopy) were not fully conclusive.⁴⁻⁶ However it is already well known that differentiation between brain abscess and high grade glioma can be very difficult because imaging characteristics from multiparametric and multimodality imaging can be inconclusive.⁴⁻⁶ Thus, further imaging modalities aiding in ascertaining the correct diagnosis are of clinical interest.

We acquired APTw images of the patients' brain. APTw is a molecular imaging technique⁷ that has shown promise in differentiating infective mass lesions from tumorous lesions.^{7,21} In the future, APTw imaging may become a valuable asset in imaging infective mass lesions and imaging characteristics as described in this report may become of interest.

First, APTw values (maximum, mean, minimum) were higher in the direct perifocal edema surrounding the contrast enhancing rim of the *Nocardia* abscess compared to the APTw values of the contrast enhancing rim itself. This may reflect the fact that

perifocal cerebritis surrounding the real abscess area is present as can be observed by faint contrast enhancement surrounding the abscess rim (Figure 1G–1H).

Second, the necrotic central part of the brain abscess had lower APTw values compared to the contrast enhancing parts but higher values compared to normal appearing white matter. These imaging characteristics differ from those of tumorous lesions as reported in previous studies, where the mean APTw value was described to be significantly lower in the necrotic region of high grade tumors or radiation necrosis compared to healthy contralateral regions.^{22,23} It can be suspected that in infectious necrotic areas the presence of inflammatory cells leads to increased protein and peptide content,²⁴⁻²⁶ and thus to increased APTw values compared to necrotic tumorous areas.

As for the contrast enhancing rim, the values in our patient were in the same range as those reported for metastatic and primary high grade brain tumors.²⁶

Lastly, we observed two slight peaks in the histogram of the contrast enhancing rim of the brain abscess at APTw values of 2.4 and 2.9%. As these peaks have not been described for tumorous lesions, we speculate that they may potentially be specific for infective brain abscesses or even abscesses caused by *Nocardia*.²³⁻²⁸

In conclusion, we suspect that APTw imaging may provide additional insights in complex cases where multimodality and multiparametric MR imaging with DTI, PWI and spectroscopy is inconclusive. However, it has to be strongly emphasized, that the imaging characteristics described in the present work are only based on the imaging study of a single patient. Thus, future studies based on larger patient series should evaluate the utility and added value of APTw imaging in the imaging of infective mass lesions.

LEARNING POINTS

1. The diagnosis of a cerebral nocardiosis abscess may be very challenging, even when images from multimodality MR imaging are available.
2. Cerebral nocardiosis abscesses may mimic the appearance of tumorous lesions on images obtained from multimodality MR imaging.
3. APTw imaging showed distinct imaging characteristics of the brain abscess. APTw may possibly be a useful tool to differentiate tumorous lesions from pyogenic brain abscesses.

REFERENCES

1. Shirani K, Mohajeri F. *Nocardia farcinica* isolated meningitis in a patient with Behçet's disease: case report and literature review. *Rev Esp Quimioter* 2019; **32**: 381–3.
2. Uneda A, Suzuki K, Okubo S, Hirashita K, Yunoki M, Yoshino K. Brain abscess caused by *Nocardia asiatica*. *Surg Neurol Int* 2016; **7**: 74–7. doi: <https://doi.org/10.4103/2152-7806.186509>
3. Malincarne L, Marroni M, Farina C, Camanni G, Valente M, Belfiori B, et al.

- Primary brain abscess with *Nocardia farcinica* in an immunocompetent patient. *Clin Neurol Neurosurg* 2002; **104**: 132–5. doi: [https://doi.org/10.1016/S0303-8467\(01\)00201-3](https://doi.org/10.1016/S0303-8467(01)00201-3)
4. Fink JR, Muzi M, Peck M, Krohn KA. Multimodality brain tumor imaging: MR imaging, PET, and PET/MR imaging. *J Nucl Med* 2015; **56**: 1554–61. doi: <https://doi.org/10.2967/jnumed.113.131516>
 5. Tsitsia V, Svolou P, Kapsalaki E, Theodorou K, Vassiou K, Valotassiou V, et al. Multimodality-multiparametric brain tumors evaluation. *Hell J Nucl Med* 2017; **20**: 57–61.
 6. Nael K, Bauer AH, Hormigo A, Lemole M, Germano IM, Puig J, et al. Multiparametric MRI for differentiation of radiation necrosis from recurrent tumor in patients with treated glioblastoma. *AJR Am J Roentgenol* 2018; **210**: 18–23. doi: <https://doi.org/10.2214/AJR.17.18003>
 7. Wang W, Zhang H, Lee D-H, Yu J, Cheng T, Hong M, et al. Using functional and molecular MRI techniques to detect neuroinflammation and neuroprotection after traumatic brain injury. *Brain Behav Immun* 2017; **64**: 344–53. doi: <https://doi.org/10.1016/j.bbi.2017.04.019>
 8. Kumar VA, Augustine D, Panikar D, Nandakumar A, Dinesh KR, Karim S, et al. *Nocardia farcinica* Brain Abscess: Epidemiology, Pathophysiology, and Literature Review. *Surg Infect* 2014; **15**: 640–6. doi: <https://doi.org/10.1089/sur.2012.205>
 9. Beuret F, Schmitt E, Planel S, Lesanne G, Bracard S. Subtentorial cerebral nocardiosis in immunocompetent patients: CT and MR imaging findings. *Diagn Interv Imaging* 2015; **96**: 953–7. doi: <https://doi.org/10.1016/j.diii.2015.03.010>
 10. Wilson JW. Nocardiosis: updates and clinical overview. *Mayo Clinic Proceedings* 2012; **87**: 403–7. doi: <https://doi.org/10.1016/j.mayocp.2011.11.016>
 11. Toh CH, Wei K-C, Chang C-N, Hsu P-W, Wong H-F, Ng S-H, et al. Differentiation of pyogenic brain abscesses from necrotic glioblastomas with use of susceptibility-weighted imaging. *AJNR Am J Neuroradiol* 2012; **33**: 1534–8. doi: <https://doi.org/10.3174/ajnr.A2986>
 12. Toh CH, Wei K-C, Chang C-N, Ng S-H, Wong H-F, Lin C-P. Differentiation of brain abscesses from glioblastomas and metastatic brain tumors: comparisons of diagnostic performance of dynamic susceptibility contrast-enhanced perfusion MR imaging before and after mathematic contrast leakage correction. *PLoS One* 2014; **9**: e109172. doi: <https://doi.org/10.1371/journal.pone.0109172>
 13. Chiang I-C, Hsieh T-J, Chiu M-L, Liu G-C, Kuo Y-T, Lin W-C. Distinction between pyogenic brain abscess and necrotic brain tumour using 3-tesla MR spectroscopy, diffusion and perfusion imaging. *Br J Radiol* 2009; **82**: 813–20. doi: <https://doi.org/10.1259/bjr/90100265>
 14. Toh CH, Wei K-C, Ng S-H, Wan Y-L, Lin C-P, Castillo M. Differentiation of brain abscesses from necrotic glioblastomas and cystic metastatic brain tumors with diffusion tensor imaging. *AJNR Am J Neuroradiol* 2011; **32**: 1646–51. doi: <https://doi.org/10.3174/ajnr.A2581>
 15. Muccio CF, Caranci F, D'Arco E, Cerase A, De Lipsis L, Esposito G, et al. Magnetic resonance features of pyogenic brain abscesses and differential diagnosis using morphological and functional imaging studies: a pictorial essay. *J Neuroradiol* 2014; **41**: 153–67. doi: <https://doi.org/10.1016/j.neurad.2014.05.004>
 16. Rath TJ, Hughes M, Arabi M, Shah GV. Imaging of cerebritis, encephalitis, and brain abscess. *Neuroimaging Clin N Am* 2012; **22**: 585–607. doi: <https://doi.org/10.1016/j.nic.2012.04.002>
 17. De Simone M, Brogna B, Sessa G, Oliva G, Guida B, Magliulo M. Valuable contribution of magnetic resonance spectroscopy in differentiation of brain abscess from glioma. *Infect Dis* 2017; **49**(11-12): 871–3. doi: <https://doi.org/10.1080/23744235.2017.1331464>
 18. Arevalo-Perez J, Peck KK, Young RJ, Holodny AI, Karimi S, Lyo JK. Dynamic contrast-enhanced perfusion MRI and diffusion-weighted imaging in grading of gliomas. *J Neuroimaging* 2015; **25**: 792–8. doi: <https://doi.org/10.1111/jon.12239>
 19. Jia ZZ, Gu HM, Zhou XJ, Shi JL, Li MD, Zhou GF, et al. The assessment of immature microvascular density in brain gliomas with dynamic contrast-enhanced magnetic resonance imaging. *Eur J Radiol* 2015; **84**: 1805–9. doi: <https://doi.org/10.1016/j.ejrad.2015.05.035>
 20. Choi HS, Kim AH, Ahn SS, Shin N-young, Kim J, Lee S-K. Glioma grading capability: comparisons among parameters from dynamic contrast-enhanced MRI and ADC value on DWI. *Korean J Radiol* 2013; **14**: 487–92. doi: <https://doi.org/10.3348/kjr.2013.14.3.487>
 21. Debnath A, Gupta RK, Singh A. Evaluating the Role of Amide Proton Transfer (APT)–Weighted Contrast, Optimized for Normalization and Region of Interest Selection, in Differentiation of Neoplastic and Infective Mass Lesions on 3T MRI. *Mol Imaging Biol* 2019; **15**. doi: <https://doi.org/10.1007/s11307-019-01382-x>
 22. Jiang S, Yu H, Wang X, Lu S, Li Y, Feng L, et al. Molecular MRI differentiation between primary central nervous system lymphomas and high-grade gliomas using endogenous protein-based amide proton transfer MR imaging at 3 tesla. *Eur Radiol* 2016; **26**: 64–71. doi: <https://doi.org/10.1007/s00330-015-3805-1>
 23. Jiang S, Rui Q, Wang Y, Heo H-Y, Zou T, Yu H, et al. Discriminating MGMT promoter methylation status in patients with glioblastoma employing amide proton transfer-weighted MRI metrics. *Eur Radiol* 2018; **28**: 2115–23. doi: <https://doi.org/10.1007/s00330-017-5182-4>
 24. Wen Z, Hu S, Huang F, Wang X, Guo L, Quan X, et al. Mr imaging of high-grade brain tumors using endogenous protein and peptide-based contrast. *Neuroimage* 2010; **51**: 616–22. doi: <https://doi.org/10.1016/j.neuroimage.2010.02.050>
 25. Zhou J, Tryggstad E, Wen Z, Lal B, Zhou T, Grossman R, et al. Differentiation between glioma and radiation necrosis using molecular magnetic resonance imaging of endogenous proteins and peptides. *Nat Med* 2011; **17**: 130–4. doi: <https://doi.org/10.1038/nm.2268>
 26. Yu H, Lou H, Zou T, Wang X, Jiang S, Huang Z, et al. Applying protein-based amide proton transfer MR imaging to distinguish solitary brain metastases from glioblastoma. *Eur Radiol* 2017; **27**: 4516–24. doi: <https://doi.org/10.1007/s00330-017-4867-z>
 27. Sartoretti T, Sartoretti E, Wyss M, Á S, Najafi A, Binkert C, et al. Amide proton transfer contrast distribution in different brain regions in young healthy subjects. *Front Neurosci* 2019; **22**: 520.
 28. Sartoretti E, Sartoretti T, Wyss M, Becker AS, Schwenk Árpád, van Smoorenburg L, et al. Amide proton transfer weighted imaging shows differences in multiple sclerosis lesions and white matter hyperintensities of presumed vascular origin. *Front Neurol* 2019; **10**: 1307. doi: <https://doi.org/10.3389/fneur.2019.01307>